Available online at www.sciencedirect.com

ScienceDirect

Procedia IUTAM 19 (2016) 83 – 90

Procedia IUTAM

www.elsevier.com/locate/procedia

IUTAM Symposium Analytical Methods in Nonlinear Dynamics

Detecting the Shilnikov scenario in a Hopf-Hopf bifurcation with 1:3 resonance

Alois Steindl

TU Wien
Institute for Mechanics and Mechatronics
Getreidemarkt 9
1060 Vienna, Austria

Abstract

We investigate the behaviour of the primary solutions at a Hopf-Hopf interaction close to a 1:3 resonance. It turns out, that the secondary bifurcations from the primary periodic solution branches are governed by Duffing and Mathieu equations.

By numerical path following a homoclinic orbit at a saddle node was detected, giving rise to the Shilnikov scenario. In order to understand the creation of homoclinic orbits, a continuation of that orbit was applied, which terminated at an equilibrium with a triple zero eigenvalue. The existence of different types of homoclinic and heteroclinic orbits in the vicinity of triple zero bifurcation points has already been established. A short discussion of the local bifurcations at the triple zero eigenvalue is given.

Keywords: Hopf-Hopf bifurcation; resonance; Shilnikov scenario; Duffing equation; Mathieu equation; Homoclinic orbit; triple zero eigenvalue

1. Introduction

During the investigation of oscillatory systems Hopf-Hopf mode interactions occur quite frequently and may already give rise to interesting dynamics, like 3-frequency tori or heteroclinic orbits, which indicate small-scale chaotic behaviour in the non-averaged system. If further parameters are varied, low order resonances can occur, increasing the possibility of complicated solution patterns.

A mechanical model with a rich bifurcation structure is given by a fluid conveying tube[1], which is supported at the position $s = \xi\ell$ by a linear spring of stiffness c. A typical stability chart of the straight downhanging equilibrium is displayed in Fig. 1: If the flow rate ϱ increases, either a zero eigenvalue (dashed curve) is encountered for large values of c, leading to a buckling of the tube, or a pair of imaginary eigenvalues $\sigma = \pm i\omega$ (solid curve) is found for smaller stiffness c. For the chosen parameter values the Hopf bifurcation curve intersects the curve with $\sigma = 0$ in

* Corresponding author. Tel.: +43-1-58801-325208 ; fax: +43-1-58801-9325208.
E-mail address: Alois.Steindl@tuwien.ac.at

doi:10.1016/j.piutam.2016.03.012

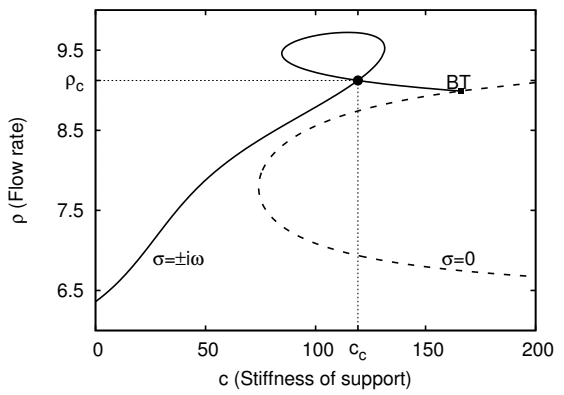

Fig. 1. Stability boundaries in (c, ϱ)-parameter space for an elastically supported fluid conveying tube.

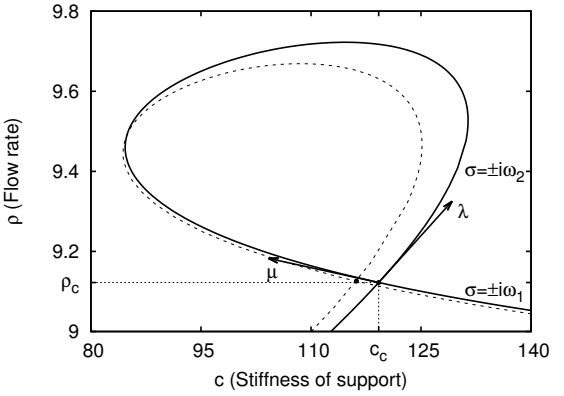

Fig. 2. Variation of the stability boundary for a slightly changed support position ξ.

a Bogdanov-Takens point ("BT"), where the purely imaginary eigenvalues $\sigma = \pm i\omega$ coalesce at the non-semisimple double eigenvalue zero. The Hopf bifurcation curve forms a loop and intersects itself at the point (c_c, ϱ_c): If the stiffness c is fixed at c_c, two pairs of purely imaginary eigenvalues occur at $\varrho = \varrho_c$ simultaneously. For a certain value ($\xi_r \approx 0.88634$) of the parameter ξ the imaginary parts satisfy the resonance condition $\omega_2 = 24.8076 = 3\omega_1$. In Fig. 2 the Hopf bifurcation boundaries for $\xi = \xi_r$ and $\xi = \xi_r + 0.001$ (dashed curve) are displayed close to the resonant Hopf-Hopf interaction. For $\xi = \xi_r + 0.001$ the bifurcation boundary intersects itself close to (c_c, ϱ_c); the purely imaginary eigenvalues $\pm i\omega_j$ at this point satisfy

$$\omega_1 = 8.63917, \quad \omega_2 = 24.5399, \quad \delta = \omega_2 - 3\omega_1 = -1.37757.$$

In Fig. 2 also the directions of the mathematical unfolding parameters λ and μ are displayed. They are tangent to the stability boundaries at the intersection points and point in the direction of increasing real parts of the eigenvalues.

A combined analytical and numerical investigation of the 1:2 and 1:3 resonances was carried out in Ref.[4], displaying a rich solution scenario in the vicinity of the bifurcation point. While in the non-resonant case the secondary bifurcations create tori, the secondary branches in the resonant case also contain transitions between periodic and quasiperiodic solutions.

The focus of the investigations in the first part will be the stability loss of the primary solution branches. It turns out, that the slow oscillation also excites the higher harmonics, whose dynamics is governed by a Duffing equation, whereas the the bifurcation from the fast oscillation is governed by a nonlinear Mathieu-type equation.

During the path-following of a periodic solution in the reduced problem a homoclinic orbit was observed, which gives rise to a Shilnikov scenario. Originally we supposed that this homoclinic orbit is related to the heteroclinic orbit between the primary branches in the non-resonant system. Performing a continuation of the homoclinic orbit in the unfolding parameters, the branch ended up in the vicinity of a bifurcation with a threefold zero eigenvalue. The occurence of homoclinic and heteroclinic solutions close to the triple zero bifurcation was already shown in[3] and[2]. In the final section of this article a short discussion of the threefold zero bifurcation will be given.

2. Normal Form equations for the Hopf-Hopf interaction with 1:3 resonance.

The third order normal form equations of the unfolded system close to a 1:3 resonant Hopf bifurcation are given by the complex equations[7]

$$\dot{z}_1 = (\lambda + i\omega)z_1 + A_1|z_1|^2 z_1 + A_2|z_2|^2 z_1 + A_3\bar{z}_1^2 z_2, \tag{1a}$$

$$\dot{z}_2 = (\mu + 3i\omega + i\delta)z_2 + A_4|z_1|^2 z_2 + A_5|z_2|^2 z_2 + A_6 z_1^3, \tag{1b}$$

where λ, μ, and δ are the unfolding parameters and the complex valued coefficients $A_j = c_j + id_j$ are obtained from the cubic expansion of the system at the bifurcation point. The terms with A_1, A_2, A_4 and A_5 would also show up at a non-resonant Hopf-Hopf interaction, whereas the last terms in both equations appear due to the 1:3-resonance. Throughout this article the following values for the cubic coefficients will be used for the numerical calculations

$$A_1 = 4.03479 - 1.80535i, \qquad A_2 = 10.2064 + 5.82019i, \qquad A_3 = 0.48729 + 13.0561i,$$
$$A_4 = -14.4166 - 0.712095i, \qquad A_5 = -1.22844 + 0.0601914i, \qquad A_6 = -1.35391 + 3.9928i.$$

These values were obtained by Center Manifold reduction and Normal Form computation at an 1:3-resonance for a fluid conveying tube with elastic support and an additional mass at the lower end.

By introducing polar coordinates $z_j = r_j \exp(i\varphi_j)$ the equations (1a) and (1b) could be reduced to the three-dimensional real equations for the amplitudes r_j and the resonance angle $\psi = 3\varphi_2 - \varphi_1$

$$\dot{r}_1 = (\lambda + c_1 r_1^2 + c_2 r_2^2) r_1 + (c_3 \cos\psi - d_3 \sin\psi) r_1^2 r_2, \tag{2a}$$
$$\dot{r}_2 = (\mu + c_4 r_1^2 + c_5 r_2^2) r_2 + (c_6 \cos\psi + d_6 \sin\psi) r_1^3, \tag{2b}$$
$$\dot{\psi} = \delta + (d_4 - 3d_1) r_1^2 + (d_5 - 3d_2) r_2^2 + (d_6 \cos\psi - c_6 \sin\psi) r_1^3 / r_2 - 3(d_3 \cos\psi + c_3 \sin\psi) r_1 r_2. \tag{2c}$$

Since (2c) becomes singular for $r_2 = 0$, we introduce rotating coordinates

$$z_1(t) = \exp(i\Omega(t))\, w_1, \quad z_2 = \exp(3i\Omega(t))\, w_2, \tag{3}$$

where $\Omega(t)$ is chosen, such that $w_1(t) \in \mathbb{R}$:

$$\dot{\Omega} = \omega + d_1 |w_1|^2 + d_2 |w_2|^2 + \operatorname{Im} A_3\, \overline{w}_1^2 w_2. \tag{4}$$

With $\dot{z}_2 = \exp(3i\Omega(t))(\dot{w}_2 + 3i\dot{\Omega} w_2)$ we obtain the regular system for $w_1 = x_1$ and $w_2 = x_2 + iy_2$

$$\dot{x}_1 = (\lambda + c_1 x_1^2 + c_2 |w_2|^2) x_1 + (c_3 x_2 - d_3 y_2) x_1^2, \tag{5a}$$
$$\dot{x}_2 = (\mu + c_4 x_1^2 + c_5 |w_2|^2) x_2 - (\delta - 3\dot{\Omega} + d_4 x_1^2 + d_5 |w_2|^2) y_2 + c_6 x_1^3, \tag{5b}$$
$$\dot{y}_2 = (\delta - 3\dot{\Omega} + d_4 x_1^2 + d_5 |w_2|^2) x_2 + (\mu + c_4 x_1^2 + c_5 |w_2|^2) y_2 + d_6 x_1^3. \tag{5c}$$

Instead of (4) we could equally well have chosen the rotation, such that $w_2(t) \in \mathbb{R}$.

3. Primary solution branches

First we have a closer look at the primary solution branches, which bifurcate from the trivial state $\boldsymbol{z} = \mathbf{0}$ at the stability boundaries $\lambda = 0$ and $\mu = 0$.

3.1. Branching and stability of the slow mode solution

Along the line $\lambda = 0$ the trivial state looses its stability by a Hopf bifurcation with imaginary eigenvalues $\pm i\omega$. In the non-resonant case a pure Mode-1 solution ($z_2 = 0$) would bifurcate from the origin, but in the resonant case the term $A_6 z_1^3$ in (1b) prevents that simple solution. If μ and δ are sufficiently far from zero, we could apply Center Manifold reduction and obtain

$$z_2(t) \approx z_1^3 A_6 / (\mu + i\delta), \tag{6}$$

so $|z_2| = O(|z_1|^3$. Using this estimate in (1a) we observe, that the cubic terms containing z_2 can be savely neglected and we recover the bifurcation equation for the non-resonant problem

$$\dot{z}_1 = (\lambda + i\omega + A_1 |z_1|^2) z_1. \tag{7}$$

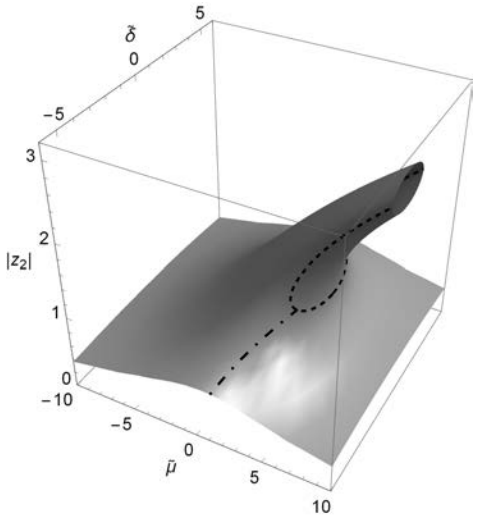

Fig. 3. Solution manifold for the bifurcation equation (9) for fixed r_1. The dashed curve indicates zero eigenvalues; along the dot-dashed curve secondary Hopf bifurcations to quasiperiodic solutions occur.

Its periodic solutions $z_1 = r_1 \exp(i\Omega_1 t)$ with $\Omega_1 = \omega + d_1 r_1^2$ satisfy the branching equation $\lambda + c_1 r_1^2 = 0$ and are supercritical and stable, if $c_1 < 0$.

In order to investigate the behaviour of this solution in the second direction, we assume, that $|z_2|$ remains sufficiently small, such that it doesn't influence (1a). Inserting the slow motion into the fast equation (1b), we obtain the equation

$$\dot{z}_2 = (\tilde{\mu} + i\tilde{\delta} + 3i\Omega_1 + A_5|z_2|^2)z_2 + A_6 z_1^3, \tag{8}$$

with the shifted parameters

$$\tilde{\mu} = \mu + c_4 r_1^2,$$
$$\tilde{\delta} = \delta + (d_4 - 3d_1) r_1^2.$$

Since the last term in (8) oscillates with angular frequency $3\Omega_1$, (8) is the equation of a Duffing oscillator with linear and non-linear damping. It's periodic solutions with angular frequency $3\Omega_1$ are obtained using the ansatz

$$z_2 = b \exp(3i\Omega_1 t - i\psi),$$

which leads to the equations

$$(\tilde{\mu} + c_5 b^2)b = -\operatorname{Re}(A_6 \exp(i\psi))r_1^3,$$
$$(\tilde{\delta} + d_5 b^2)b = -\operatorname{Im}(A_6 \exp(i\psi))r_1^3.$$

Eliminating ψ yields the equation

$$\left((\tilde{\mu} + c_5 b^2)^2 + (\tilde{\delta} + d_5 b^2)^2\right) = |A_6|^2 r_1^3, \tag{9}$$

which for fixed b describes a circle with radius $|A_6| r_1^3 / b$ and center $(-c_5 b^2, -d_5 b^2)$ in the $(\tilde{\mu}, \tilde{\delta})$ plane. The shape of the solution set of eqn. (9) is displayed in Fig. 3.

The stability of the slow periodic oscillations is determined by the coefficient c_1 in the direction of the first mode and by the Jacobian of (8)

$$\mathbf{J}_2 = \begin{pmatrix} \tilde{\mu} + i\tilde{\delta} + 2A_5|z_2|^2 & A_5 z_2^2 \\ \overline{A}_5 \overline{z}_2^2 & \tilde{\mu} - i\tilde{\delta} + 2\overline{A}_5|z_2|^2 \end{pmatrix} \tag{10}$$

in the fast direction. The trace and determinant of $\mathbf{J}_2$ are given by the real valued expressions

$$\begin{aligned}\mathrm{tr}(\mathbf{J}_2) &= 2\tilde{\mu} + 4c_5|z_2|^2,\\ \det(\mathbf{J}_2) &= \left|\tilde{\mu} + i\tilde{\delta} + 2A_5|z_2|^2\right|^2 - |A_5|^2|z_2|^4.\end{aligned}$$

Zero eigenvalues of $\mathbf{J}_2$ occur, when $\det(\mathbf{J}_2) = 0$, which happens, when the tangential plane to the solution set of (8) becomes vertical, indicated by the dashed curve in Fig. 3.

Hopf bifurcations occur, when $\mathrm{tr}(\mathbf{J}_2) = 0$ and $\det(\mathbf{J}_2) > 0$. At these points, which are shown as dot-dashed curve in Fig. 3, a quasiperiodic solution bifurcates from the slow oscillation. At the intersections of these bifurcation boundaries a Takens-Bogdanov bifurcation occurs.

3.2. Branching and stability of the fast oscillation

Along the stability boundary $\mu = 0$ the branch of fast oscillations

$$z_1 = 0, \tag{11a}$$

$$z_2 = r_2 \exp(3i\Omega_2 t) \quad \text{with } \mu + c_5 r_2^2 = 0 \quad \text{and } 3\Omega_2 = 3\omega + \delta + d_5 r_2^2 \tag{11b}$$

bifurcates from the trivial state. Its stability in the fast direction is determined by the sign of c_5. A secondary bifurcation occurs, if the Jacobian of (1a) at (11)

$$\mathbf{J}_1(0) = \lambda + i\omega + A_2|z_2|^2 \tag{12}$$

becomes unstable, that is, if $\mathrm{Re}(\mathbf{J}_1(0)) = \lambda + c_2|z_2|^2 = 0$. In the non-resonant Hopf-Hopf interaction a quasi-periodic solution would bifurcate from the periodic oscillation, but in the resonant case the last term $A_3\overline{z}_1^2 z_2$ in (1a) acts like a parametric excitation and gives (1a) the form of a nonlinear Mathieu equation for a given periodic oscillation $z_2(t)$. Therefore we should also expect periodic solutions for certain parameter values.

With the ansatz $z_1 = r_1 \exp(i\Omega_2 t - i\phi)$ and the shifted parameters

$$\begin{aligned}\tilde{\lambda} &= \lambda + c_2 r_2^2,\\ \tilde{\Delta} &= (d_2 - d_5/3)r_2^2 - \delta/3,\end{aligned}$$

we obtain the bifurcation equation

$$(\tilde{\lambda} + i\tilde{\Delta} + A_1 r_1^2)r_1 + A_3 r_1^2 r_2 \exp(3i\phi) = 0. \tag{13}$$

Dividing by r_1 and eliminating ϕ from (13) we obtain the scalar equation

$$(\tilde{\lambda} + c_1 r_1^2)^2 + (\tilde{\Delta} + d_1 r_1^2)^2 = |A_3|^2 r_1^2 r_2^2, \tag{14}$$

which for fixed values of r_1 and r_2 describes a circle of radius $|A_3|r_1 r_2$ in the $(\tilde{\lambda}, \tilde{\Delta})$-plane centered at $(-c_1 r_1^2, -d_1 r_1^2)$. The solution manifold in $(\tilde{\lambda}, \tilde{\Delta}, r_1)$-space is displayed in Fig. 4. It touches the plane $r_1 = 0$ in the point $(\tilde{\lambda}, \tilde{\Delta}) = (0, 0)$: If $\tilde{\lambda} = \lambda + c_2 r_2^2$ and $\tilde{\Delta} = (d_2 - d_5/3)r_2^2 - \delta/3$ vanish simultaneously, a family of synchronous periodic solutions is born. Otherwise a branch of quasi-periodic solutions bifurcates at $\tilde{\lambda} = 0$ from the fast periodic solution. At higher amplitudes the quasiperiodic solution connects to the family of periodic solutions.

The stability of the periodic oscillations in the first component can again be determined by the Jacobian of (14)

$$\mathbf{J}_1(w_1) = \begin{pmatrix} \tilde{\lambda} + i\tilde{\Delta} + 2A_1|w_1|^2 & A_1 w_1^2 + 2A_3\overline{w}_1 r_2 \\ \overline{A}_1\overline{w}_1^2 + 2\overline{A}_3 w_1 r_2 & \tilde{\lambda} - i\tilde{\Delta} + 2\overline{A}_1|w_1|^2 \end{pmatrix} \quad \text{with } w_1 = r_1\exp(-i\phi). \tag{15}$$

Its real valued trace and determinant are given by

$$\mathrm{tr}(\mathbf{J}_1(w_1)) = 2(\tilde{\lambda} + 2c_1 r_1^2), \tag{16a}$$

$$\det(\mathbf{J}_1(w_1)) = |\tilde{\lambda} + i\tilde{\Delta} + 2A_1|w_1|^2|^2 - |A_1 w_1^2 + 2A_3\overline{w}_1 r_2|^2. \tag{16b}$$

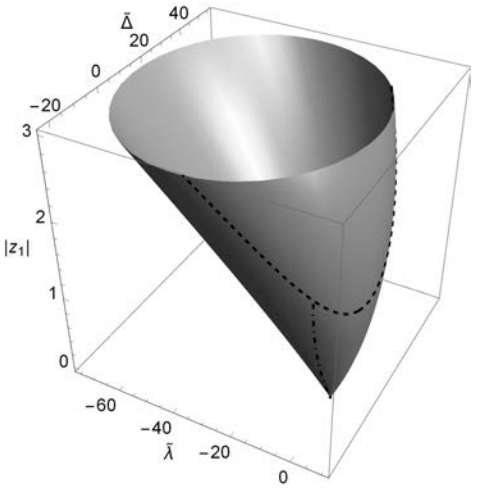

Fig. 4. Bifurcation diagram for (14) displaying the family of periodic oscillations. The dashed and dot-dashed curves indicate turning points and Hopf bifurcation points.

The location of turning points, where $\mathrm{tr}(\mathbf{J}_1(w_1))$ vanishes, is indicated by the dashed curve in Fig. 4. A Hopf bifurcation occurs, when $\mathrm{tr}(\mathbf{J}_1(w_1)) = 0$ and $\det(\mathbf{J}_1(w_1)) > 0$; it is indicated by the dot-dashed curve in Fig. 4. At the intersection of these two stability boundaries a Takens-Bogdanov bifurcation occurs. Since in our problem $c_1 > 0$, the mixed-mode periodic solution is unstable.

It should be noted, that the discussions of the mixed mode solutions are valid only for $r_2 \ll r_1$ for the Duffing scenario, and for $r_1 \ll r_2$ in the Mathieu scenario, respectively. In these two cases we could either neglect the influence of the term $A_3\bar{z}_1^2 z_2$ or $A_6 z_1^3$, resulting in a bifurcation equation, which contained one unknown angular variable, which could then be eliminated. If we allow both modes to be of comparable size, we have to deal with the full three-dimensional system and also have to investigate the three-dimensional Jacobians for the stability calculations.

3.3. Numerical observations and Shilnikov bifurcation[6]

For a set of coefficients A_j we followed the bifurcation branches of the reduced system (5) numerically using the continuation software MatCont[5]. Since we considered only cubic nonlinearities in the bifurcation equations, the system (1) is invariant under the scaling transformation

$$\lambda \mapsto \varepsilon^2\lambda, \qquad \mu \mapsto \varepsilon^2\mu, \qquad \delta \mapsto \varepsilon^2\delta,$$
$$z_i \mapsto \varepsilon z_i, \qquad t \mapsto t/\varepsilon^3.$$

Therefore we can keep one unfolding parameter constant. Since the slow mode bifurcates subcritically, we choose $\lambda = -1$. Some solution branches for fixed $\delta = 0.5$ are shown in Fig. 5: The lower equilibrium branch corresponds to the low amplitude response in the Duffing equation for the slow oscillation. The upper branch shows the large amplitude response for that case. According to Fig. 3 we would expect that this separated branch is closed, but due to the large amplitude of $|z_2|$ the Duffing approximation becomes inappropriate.

From a Hopf bifurcation along the lower branch a subcritical periodic solution emanates, corresponding to a torus in the original system (1). This branch spirals towards a certain point. Looking at the period along this branch, as it is shown in Fig. 6, we observe the typical snaking behaviour for a Shilnikov scenario: Along the branch the period T increases to infinity, while the bifurcation parameter μ converges to some fixed value. At the endpoint of this curve a homoclinic orbit of a saddle-focus instability is found: Starting along the unstable two-dimensional manifold the orbit spirals off the equilibrium point and returns along the stable one-dimensional manifold. In the vicinity of such a homoclinic orbit an infinite set of horseshoe maps can exist, leading to very chaotic dynamics. Such a homoclinic orbit was also observed in Ref.[4].

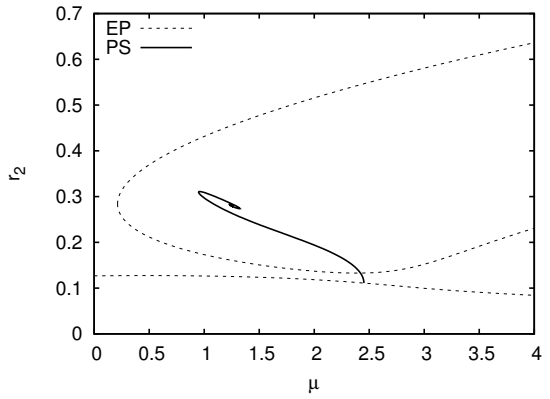

Fig. 5. Partial bifurcation diagram for (5) with $\lambda = -1$ and $\delta = 0.5$. "EP" denotes equilibrium points, "PS" denotes a periodic solution.

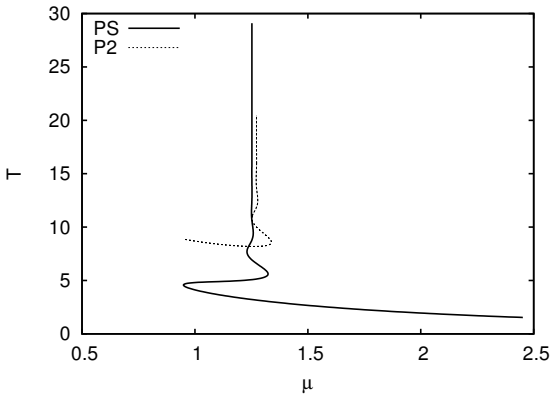

Fig. 6. Period T of the periodic solution in Fig. 5 and of a bifurcating period-2 branch.

In order to understand the occurence of this phenomenon in the 1:3 Hopf-Hopf interaction, a continuation strategy was applied for the homoclinic orbit in the (μ, δ) parameter plane. Starting at $(\mu, \delta) \approx (1.25, 0.5)$, the branch finished at $(\mu, \delta) \approx (2.72, -3.68)$, where the homoclinic orbit became very small. All three eigenvalues decreased towards 0, so we expected a steady solution with a triple zero eigenvalue at the endpoint. Since a triple zero eigenvalue requires three parameters for a generic unfolding, we had to allow a third parameter, in addition to μ and δ, to vary. Selecting λ as third parameter wouldn't help due to the scaling invariance. Therefore we introduced a scaling parameter γ, which multiplies the nonlinear resonance coefficients A_3 and A_6. For $\gamma = 1$ we have our original set of parameters, whereas for $\gamma = 0$ we would obtain the non-resonant case.

For $\gamma \approx 0.9225$ we found an equilibrium point with a threefold zero eigenvalue. This artificial point would not occur in the original system, but it can be regarded as organizing center for the observed homoclinic orbits.

3.4. Short survey of the threefold zero eigenvalue

It was shown in[2,3], that at a triple zero eigenvalue several kinds of homoclinic orbits can be found. A possible unfolding of the normal Form system at second order is given by the system

$$\dot{x} = y, \tag{17a}$$

$$\dot{y} = z, \tag{17b}$$

$$\dot{z} = \mu_0 + \mu_2 y + \mu_3 z + a_1 x^2 + a_2 xy + a_3 y^2 + a_4 xz, \tag{17c}$$

where the small parameters μ_0, μ_2 and μ_3 are the unfolding parameters of the linear system and the a_i are the normal form coefficients of the second order system. The equilibria of (17) are given by

$$x_{1,2} = \pm\sqrt{-\mu_0/a_1}, \quad y = 0, \quad z = 0,$$

for $\mu_0/a_1 < 0$. The stability of these equilibria is determined by the Jacobian

$$\mathbf{J}(x_i) = \begin{pmatrix} 0 & 1 & 0 \\ 0 & 0 & 1 \\ 2a_1 x_i & \mu_2 + a_2 x_i & \mu_3 + a_4 x_i \end{pmatrix} =: \begin{pmatrix} 0 & 1 & 0 \\ 0 & 0 & 1 \\ \nu_1 & \nu_2 & \nu_3 \end{pmatrix}. \tag{18}$$

In the three-dimensional vicinity (ν_1, ν_2, ν_3) of the origin, the following bifurcation boundaries of co-dimension 2 can be found:

- $\nu_1 = \nu_2 = 0$: Bogdanov-Takens points,

- $\nu_1 = \nu_3 = 0$, $\nu_2 > 0$: Zero-Hopf points.

For the appearence of homoclinic orbits also the case $\nu_3 = 0$ plays an interesting role, because in that case the flow is volume preserving and the equilibria are of saddle-focus type. Along the homotopy path of the homoclinic orbit towards the triple zero bifurcation point that condition was fulfilled very well.

For the simplified system $a_2 = a_3 = a_4 = 0$, an exact homoclinic orbit could be constructed in Ref.[2]. By a numerical continuation from this solution, different kinds of homoclinic orbits could be found. It would be interesting to find more of these observed orbits also in the resonant Hopf-Hopf interaction.

4. Conclusions

For a Hopf-Hopf bifurcation with 1:3 resonance the branching behaviour and stability of the primary solution branches was considered. It could be shown, that the behaviour close to the slow solution mode can be modelled as a Duffing equation with nonlinear damping. The bifurcation from the fast mode is governed by a nonlinear Mathieu equation close to the resonance.

During the numerical investigation of the system a homoclinic solution for a saddle-focus equilibrium was found. This solution could be continued to a homoclinic orbit close to an equilibrium with a triple zero eigenvalue, for which the occurence of homoclinic orbits has already been established.

References

1. Albrecht, B.; Steindl, A.; Troger, H.: Non-linear Three-dimensional Oscillations of Fluid Conveying Viscoelastic Tubes with an Additional Mass, IUTAM-Symposium on Recent Developements in Non-linear Oscillations of Mechanical Systems (Nguyen Van Dao and E.J.Kreuzer eds.), SOLID MECHANICS AND ITS APPLICATIONS vol. 77, Kluwer Academic Publishers, Dortrecht 2000, 291-300.
2. Algaba, A.; Freire, E.; Gamero, E.; Rodríguez-Luis, A.J.: An exact homoclinic orbit and its connection with the Rössler system. Physics Letters A 379: 1114-1121, 2015
3. Dumortier, F.; Ibnez, S.; Kokubu, H.: New aspects in the unfolding of the nilpotent singularity of codimension three. Dynamical Systems, 16:1, 63-95, 2001. DOI:10.1080/02681110010017417
4. Luongo, A.; Paolone, A.; Di Egidio, A.: Multiple Timescales Analysis for 1:2 and 1:3 Resonant Hopf Bifurcations. Nonlinear Dynamics, 34: 269-291, 2003
5. Dhooge A., Govaerts W. and Kuznetsov Yu. A.: MatCont: A MATLAB package for numerical bifurcation analysis of ODEs. ACM TOMS 29:141–164, 2003
6. Shilnikov, L.P.: A case of the existence of a denumerable set of periodic motions Sov. Math. Dokl. 6, 163–166, 1965
7. Wiggins, S.: Introduction to Applied Nonlinear Dynamical Systems and Chaos Springer-Verlag, New York, 1990.